Automotive Brake Squeal Analysis Using a Complex Modes Approach

Summary

A methodology to study friction-induced squeal in a complete automotive disc brake assembly is presented. The analysis process uses a nonlinear static simulation sequence followed by a complex eigenvalue extraction to determine the dynamic instabilities that are manifested as unwanted noise. The effects of assembly loads; nonuniform contact pressure between the brake linings and disc; velocity-, temperature-, and pressure-dependent friction coefficients; friction-induced damping; and lining wear can be included. The methodology is demonstrated with a representative disc brake assembly. Good correlation between the analysis results and available experimental data is achieved.

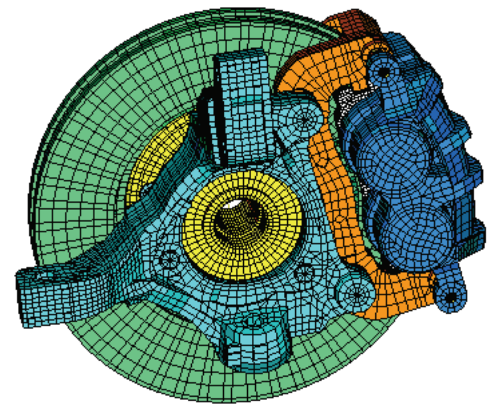

Background

The operating principle of an automobile disc brake system is to slow a moving vehicle by pressing brake pads against rotating wheel discs. The friction between the pad linings and the disc dissipates the energy of the moving vehicle, resulting in deceleration.

During brake operation, the friction between the lining and the disc can induce a dynamic instability in the system. This instability can create noise, commonly known as brake squeal. One possible explanation for the brake squeal phenomenon is the coupling of two neighboring vibration modes. If two modes are close to each other in the frequency range and have similar characteristics, they may merge if the coefficient of friction between the pad and disc increases. When these modes merge at the same frequency (become coupled), one of them becomes unstable. The unstable mode can be identified during complex eigenvalue extraction because the real part of the eigenvalue corresponding to an unstable mode is positive. The instability in the brake system design can be eliminated by changing the geometry or material properties of the brake components to decouple the modes.

As vehicle quality improves, customers demand quieter brakes. Customer complaints result in significant warranty costs yearly, motivating the need to study brake squeal early in the design process. The complex modes approach is a common finite element modeling technique used to simulate this phenomenon (e.g., Ref. 1–11).

Abaqus affords a straightforward brake squeal analysis methodology. The process consists of preloading the brake, rotating the disc, extracting natural frequencies, and computing complex eigenvalues. The approach combines all steps in one analysis and accounts for friction coupling and nonlinear effects without the need for matrix input methods or matching meshes.

Key Abaqus Features and Benefits

- Ability to use a single model for the entire analysis sequence
- The inclusion of nonlinear effects in the extraction of the complex eigenmodes
- Ability to model each part of the brake assembly independently, without the need for matching meshes

The purpose of the analysis presented here is to demonstrate the methodology by identifying any potentially unstable modes in a particular disc brake system.

Finite Element Analysis Approach

The disc brake model under consideration is shown in Figure 1. It is representative of systems used in domestic passenger vehicles and consists of a disc, two pads positioned on both sides of the disc, pad springs, knuckle, hub, carrier (or anchor bracket), pistons, and caliper housing. Contact is defined throughout the model using a small-sliding formulation. Initially the friction coefficient between the linings and disc is set to zero. The brake squeal analysis using the complex modes approach follows.

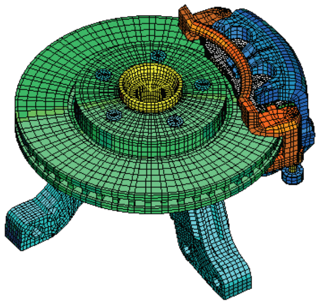

Figure 1: Disc brake model.

Step 1: Bolt pre-tension and spring interference fit analysis

In the first analysis step the model is brought into its assembled state. Fastening forces are introduced in all the bolts, and a shrink-fit procedure is used to determine the assembled state of the springs that secure the brake pads in the assembly. Figure 2 displays a close-up view of a pad retention spring after the shrink-fit procedure.

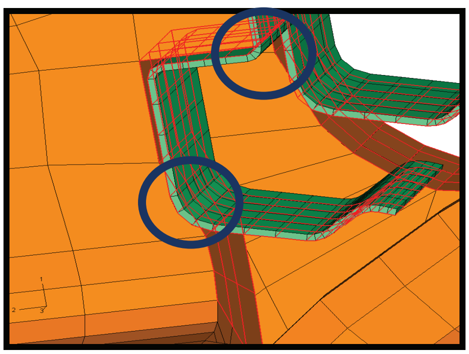

Figure 2: Shrink-fit of a brake pad spring.

Step 2: Establish disc/brake pad contact

Figure 3 displays the caliper housing and a piston. In Step 2 pressure is applied on the pistons and housing in a static analysis. The contact between the pad lining and the disc is, thus, established. Step 2 allows the contact pressure distribution on the lining surface to be determined when the disc is not rotating.

Step 3: Establish steady-state rotational motion

In this static step a rotational velocity is imposed on the disc as a predefined field variable. This provides for the modeling of steady-state frictional sliding between two bodies that are moving with different velocities. The imposed velocity of 9.26 rad/s corresponds to braking at low velocity. In addition, the friction coefficient μ is increased to 0.4 from 0.0. The present analysis uses a constant value of μ. In general, however, the friction coefficient can be defined as a function of the relative velocity (slip rate), contact pressure, and temperature. If the friction coefficient depends on the slip rate, the rotational velocity imposed is used to determine the corresponding value of μ.

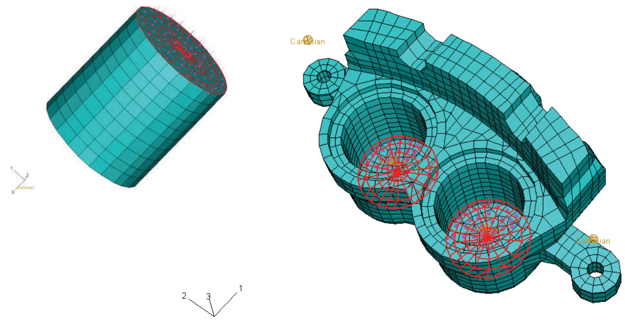

Figure 3: Caliper and piston, with pressure-loaded surfaces highlighted.

The friction coefficient is ramped up from zero to the desired value to avoid the discontinuities and convergence problems that may arise because of the change in the friction coefficient that typically occurs when bodies in contact are moving with respect to each other.

At the end of this step a steady-state braking condition is obtained. A matched mesh between the disc and the pad is not required, and a fine mesh is not required for the whole disc; rather, it is needed only in the region where the pad makes contact (see Figure 4).

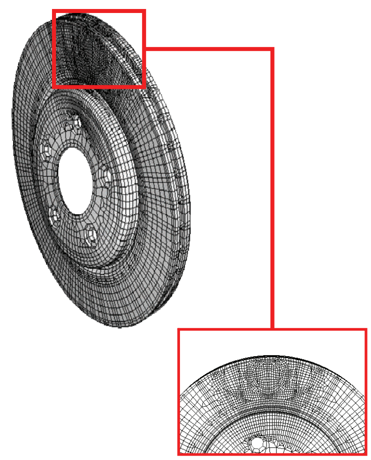

Figure 4: Disc mesh, showing refinement under pad contact area.

Step 4: Extraction of real eigenvalues and mode shapes

The preceding steps determine the initial stresses in the model and the steady-state braking conditions. In Step 4 the real eigenvalues and mode shapes of the model are extracted. In this procedure the tangential degrees of freedom at the contact nodes, at which a velocity differential is defined, are not constrained. The set of eigenmodes provides the subspace for computing complex eigenvalues in the next step.

Step 5: Extraction of complex eigenvalues and mode shapes

The complex modes analysis determines the complex eigenvalues based on the real frequency spectrum calculated in Step 4. The complex modes analysis is performed up to 10 kHz. Although not considered in the present analysis, this procedure can account for friction-induced damping.

Results

Some representative results from each analysis step follow. Figure 5 shows the Mises stress distribution on the surface of the disc due to the bolt fastening simulated in Step 1. The axial force of the bolts is specified as 2 kN, and all bolts are tightened simultaneously.

The surface pressure distribution on the brake linings after the application of pressure in Step 2 is shown in Figure 6a and Figure 6b. The accuracy of the complex mode calculation depends strongly on the accuracy of the surface pressure distribution between the pad and the disc.

After the rotational velocity is applied to the disc and the friction coefficient between the disc and the linings is increased in Step 3, the surface pressure distribution on the linings changes to that shown in Figure 7a and Figure 7b.

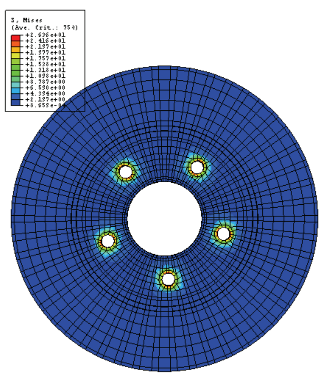

Figure 5: Mises stress distribution in the disc after bolt tightening.

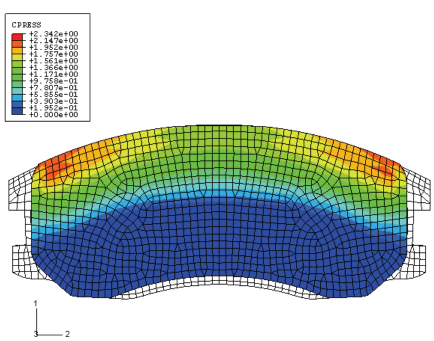

Figure 6a: Contact pressure distribution on the outboard lining at the end of Step 2.

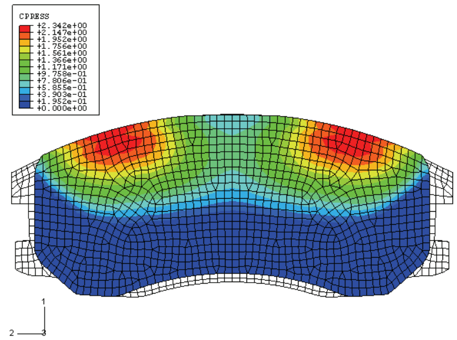

Figure 6b: Contact pressure distribution on the inboard lining at the end of Step 2.

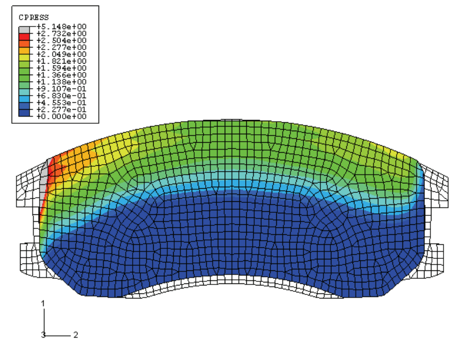

Figure 7a: Contact pressure distribution on the outboard lining at the end of Step 3.

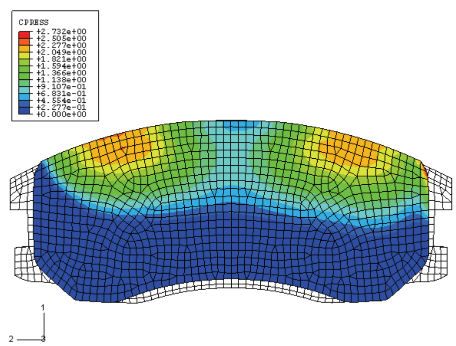

Figure 7b: Contact pressure distribution on the inboard lining at the end of Step 3.

When the real part of a complex eigenvalue becomes positive for a given set of operational parameters, the corresponding mode becomes unstable and has the potential to radiate squeal noise. An unstable mode is, thus, referred to as a squeal mode.

The disc brake system being modeled has been tested experimentally. The effects of two parameters, the caliper pressure and the friction coefficient, on the unstable modes were studied.

Figure 8 displays the real parts of the complex eigenvalues determined when the coefficient of friction is set to 0.4 and the caliper pressure is set to 1.5 MPa.

Two frequency bands, corresponding to the experimentally observed squeal frequencies, are also included in the figure.

It is clear from Figure 8 that the predicted squeal modes are included in those observed in the experiment.

As part of an experimental study presented in Abendroth et al. (Ref. 12), an electronic speckle pattern interferometry technique is used to measure the deflected shapes of a disc brake system. The system of Abendroth et al. (Ref. 12) differs slightly from that currently being simulated but still allows for meaningful comparisons.

As displayed in Figure 9, the experimentally measured shapes and the predicted shapes for the low frequency squeal mode show similarity. This mode is associated with out-of-plane disc motion coupled with pad modes. The high frequency squeal mode is dominated by tangential motion (Figure 10, next page) in which the disc exhibits predominantly in-plane rotational action.

It is natural to assume that the modes with the largest real part of an eigenvalue are likely to be unstable. However, sometimes such modes are over predictions and unstable modes with lower values of the real part can be the actual squeal modes. A preferred approach to calibrating analytical models is to start with the experimental data, identify an unstable mode of interest, and look for it among predicted instabilities.

Although not considered in the present analysis, Bajer et al. (Ref. 11) reviewed the effects of lining wear on the brake squeal predictions. The wearing effect causes the nodes at the contact surface to move by just a small amount, but the difference in the contact pressure distribution on the linings is very significant. The improved contact pressure prediction results in improved squeal mode correlation with the experimental data.

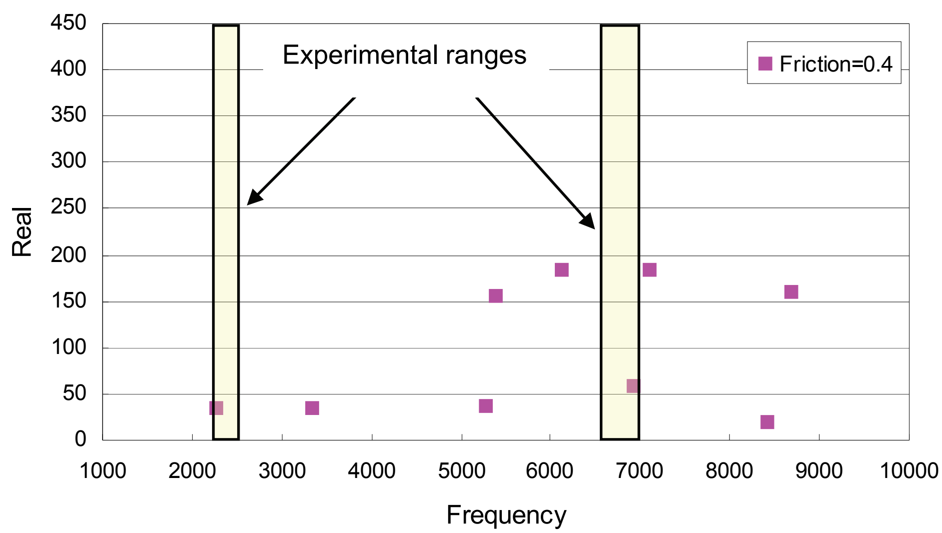

Figure 8: The predicted squeal modes at 2.2 kHz and 6.9 kHz lie in the bands (2.2–2.4 kHz and 6.6–7.0 kHz) observed experimentally.

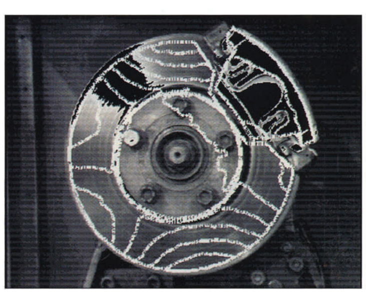

Brake disc vibration at 2.1 kHz and 18 rpm using electronic speckle pattern interferometry

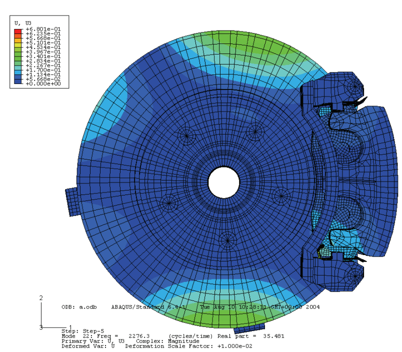

Figure 9: Mode shapes of the unstable mode at 2.2 kHz. The snapshot from the test (left) shows the mode shape when the squeal noise occurs.

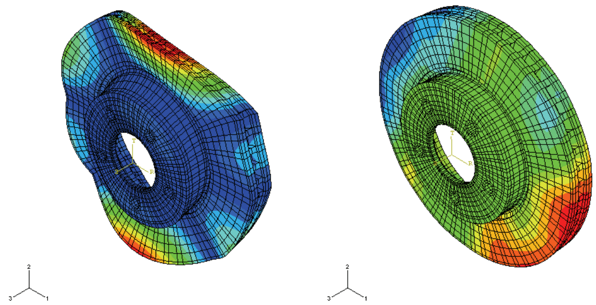

Figure 10: Mode shape of the unstable modes at 2.2 kHz (left) and 6.9 kHz (right). The high frequency contour is in a cylindrical coordinate system and shows circumferential displacement magnitude

Acknowledgements

The authors would like to thank the MANDO Corporation and SIMULIA Korea for providing the materials discussed in this article.

References

1. Liles, G. D., "Analysis of Disc Brake Squeal Using Finite Element Methods," SAE Paper 891150.
2. Nack, W. V., and A. M. Joshi, "Friction Induced Vibration: Brake Moan," SAE Paper 951095.
3. Hamzeh, O. N., W. Tworzydlo, H. J. Chang, and S. Fryska, "Analysis of Friction-Induced Instabilities in a Simplified Aircraft Brake," SAE Brake Colloquium, 1999.
4. Kung, S.-W., K. B. Dunlap, and R. S. Ballinger, "Complex Eigenvalue Analysis for Reducing Low Frequency Squeal," SAE Paper 2000-01-0444.
5. Moirot, F. C., A. Nehme, and Q. C. Nguyen, "Numerical Simulation to Detect Low-Frequency Squeal Propensity," SAE Paper 2000-01-2767.
6. Shi, T. S., O. Dessouki, T. Warzecha, W. K. Chang, and A. Jayasundera, "Advances in Complex Eigenvalue Analysis for Brake Noise," SAE Paper 2001-01-1603.
7. Lee, L., K. Xu, B. Malott, M. Matsuzaki, and G. Lou, "A Systematic Approach to Brake Squeal Simulation Using MacNeal Method," SAE Paper 2002-01-2610.
8. Ouyang, H.-J., W. V. Nack, Y. Yuan, and F. Chen, "On Automotive Disc Brake Squeal-Part II: Simulation and Analysis," SAE Paper 2003-01-0684.
9. Bajer, A., V. Belsky, and L.-J. Zeng, "Combining a Nonlinear Static Analysis and Complex Eigenvalue Extraction in Brake Squeal Simulation," SAE Paper 2003-01-3349.
10. Kung, S.-W., G. Stelzer, V. Belsky, and A. Bajer, "Brake Squeal Analysis Incorporating Contact Conditions and Other Nonlinear Effects," SAE Paper 2003-01-3343.
11. Bajer, A., V. Belsky, and S.-W. Kung, "The Influence of Friction-Induced Damping and Nonlinear Effects on Brake Squeal Analysis," SAE Paper 2004-01-2794.
12. Abendroth, H., "Advances in Brake NVH Test Equipment," Automotive Engineering International, pp. 60, February 1999.

Abaqus References

For additional information on the Abaqus capabilities referred to in this brief, see the following Abaqus Version 6.7 documentation references:

- Analysis User's Manual
  - "Static stress analysis," Section 6.2.2
  - "Natural frequency extraction," Section 6.3.5
  - "Complex eigenvalue extraction," Section 6.3.6
- Example Problems Manual
  - "Brake squeal analysis," Section 2.2.5